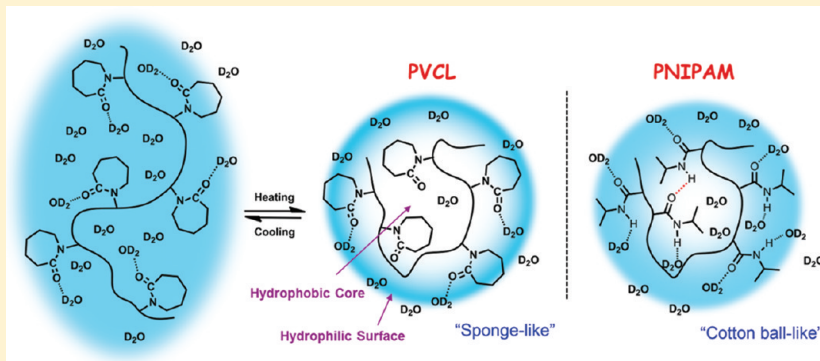


Infrared Spectroscopic Insight into Hydration Behavior of Poly(*N*-vinylcaprolactam) in Water

Shengtong Sun and Peiyi Wu*

The Key Laboratory of Molecular Engineering of Polymers, Ministry of Education, Department of Macromolecular Science, and Laboratory of Advanced Materials, Fudan University, Shanghai 200433, People's Republic of China

ABSTRACT:

IR spectroscopy in combination with two-dimensional correlation spectroscopy (2DCOS) and the perturbation correlation moving window (PCMw) technique is employed to illustrate the dynamic hydration behavior of poly(*N*-vinylcaprolactam) (PVCL) in water, which exhibits a typical type I continuous lower critical solution temperature (LCST) behavior. PCMw easily determined the transition temperature to be ca. 43.5 °C during heating and ca. 42.5 °C during cooling and the transition temperature range to be 39.5–45 °C. On the other hand, 2DCOS was used to discern the sequence order of different species in PVCL and concluded that hydrogen bonding transformation predominates at the first stage below LCST while hydrophobic interaction predominates at the second stage above LCST. In combination with molecular dynamics simulation results, we find that there exists a distribution gradient of water molecules in PVCL mesoglobules ranging from a hydrophobic core to a hydrophilic surface. Due to the absence of self-associated hydrogen bonds and topological constraints, PVCL mesoglobules would form a “sponge-like” structure which can further continuously expel water molecules upon increasing temperature, while poly(*N*-isopropylacrylamide) (PNIPAM) with self-associated hydrogen bonds forms mesoglobules with a “cotton-ball-like” structure without an apparent distribution gradient of water molecules and does not change much upon increasing temperature.

1. INTRODUCTION

Stimuli-responsive polymers, or smart polymers, capable of responses to various external stimuli (temperature, pH, pressure, etc.), represent one of the most exciting and emerging areas of scientific interest.¹ Among temperature-responsive polymers, synthetic polymers possessing a lower critical solution temperature (LCST) in aqueous solution have attracted tremendous attention due to their potential applications in controlled drug delivery,² tissue engineering,³ bioseparation,⁴ etc. Upon heating to above their LCSTs, these polymers undergo a coil-to-globule phase transition and can recover to the original state in the cooling process. Additionally, as an ideal analogue of biomolecules, research on polymers with LCST behavior is very helpful for understanding the denaturation of proteins and enzymes.

Despite the apparent similarities among various temperature-responsive water-soluble polymers, three types of LCST behavior can be distinguished according to their critical miscibility behaviors.^{5–7} Type I follows the “classical” Flory–Huggins miscibility behavior;

that is, by increasing the chain length of the polymer, the position of the critical point shifts toward lower concentration. Type II has the critical points independent of the polymer chain length. Type III is characterized by one zero limiting critical concentration and two off-zero limiting critical concentrations. Both poly(*N*-isopropylacrylamide) (PNIPAM)^{8–13} and poly(vinyl methyl ether) (PVME),^{14–16} belonging to type II and type III respectively, exhibit discontinuous phase transition behavior and have been investigated much in recent years. As a typical example of type I, poly(*N*-vinylcaprolactam) (PVCL) shows a continuous phase transition behavior, and the LCST ranges from 30 to 50 °C, strongly dependent on concentration and molecular weight.^{7,17} Although most of the environmentally sensitive polymer-based materials investigated so far are based on PNIPAM homo- and copolymers,^{18–20} PVCL has a remarkable advantage because it

Received: July 25, 2011

Revised: September 1, 2011

Published: September 07, 2011

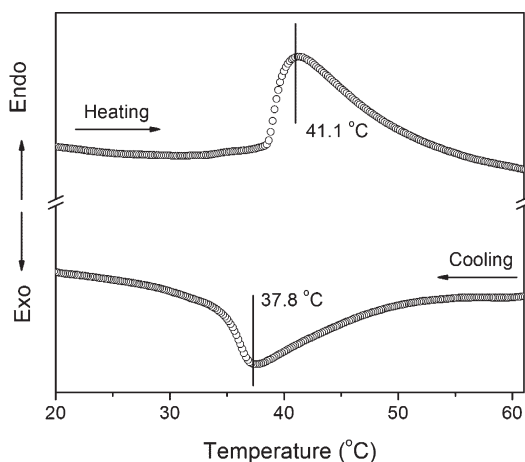


Figure 1. DSC curves of PVCL in D_2O (10 wt %) upon heating and cooling at a scanning rate of $10\text{ }^\circ\text{C}/\text{min}$.

does not produce toxic low-molecular-weight amines during hydrolysis,²¹ which has been proven by cytotoxicity evaluation.²² Owing to their excellent biocompatibility and temperature sensitivity, PVCL-based materials such as copolymers,^{23–25} hydrogels,^{26,27} microgels,^{28–30} multilayers,^{31,32} and organic/inorganic nanohybrids^{33–35} have been widely used in controlled drug release,³⁶ the immobilization of enzymes and cells,³⁷ fluorescent thermometers,³⁸ and stationary phases for liquid chromatography.³⁹ For example, the incorporation of hydrophilic imidazole units into PVCL chains would produce “protein-like” polymers which are still soluble in the globular state without macroscopic phase separation.^{40,41}

Large numbers of investigations have been devoted to account for the hydration behavior of PVCL chains. Lau and Wu found a novel way to estimate the Flory Θ -temperature ($\sim 29.5\text{ }^\circ\text{C}$) of high-molecular-mass PVCL chains from the temperature and concentration dependence of the hydrodynamic radius.⁴² Due to the rather low latent heat of transition (-1.7 kJ/mol), hydrated PVCL macromolecules may be used as highly sensitive detectors of water associates and interactions, which are affected by the polarization action of high polar amide $\text{C}=\text{O}$ groups and by specific configurational and conformational structures.^{43,44} Additionally, the colloidal mesoglobules formed by PVCL linear chains were proven to be stable for several days due to the presence of the hydrophilic outer surface.^{45,46} Fluorescence and small-angle neutron scattering (SANS) investigations showed that PVCL undergoes a conformational change from an expanded coil to a compact globule at its LCST, but with a reducing magnitude compared to PNIPAM.^{47,48} According to absorption millimeter-wave measurements, the association of hydrophobic groups in PVCL upon coil-to-globule transition causes an apparent decrease in the relative hydration number.⁴⁹ Some theoretical models^{50–52} have also been proposed to interpret the competition of the hydrophobic and hydrophilic effects of PVCL, e.g., the simplest HP side-chain model⁵⁰ of an amphiphilic polymer consisting of hydrophobic (H) strings and hydrophilic (P) beads. However, the also-existing hydrophobic groups in side chains of PVCL make the case more complicated. Generally, due to the absence of strong self-associated hydrogen bonds compared to PNIPAM in the globular state, hydrophobic hydration was considered to be predominant in the type I continuous phase transition of PVCL in aqueous solution.^{53,54}

As we know, IR is rather sensitive to morphology and conformational changes by reflecting subtle information at the molecular level. Up to now, although plenty of IR studies have been reported on the hydration behavior of PNIPAM^{10–12,55–57} and PVME,^{14,15} very few IR investigations¹⁷ were focused on the hydration behavior of PVCL. Especially noteworthy, the thermodynamic nature of the continuous phase transition of PVCL has never been clarified, wherein the respective contributions of hydrogen bonding and hydrophobic interaction should be clearly understood. In this paper, we attempt to employ two-dimensional correlation spectroscopy (2DCOS)^{58,59} in combination with the perturbation correlation moving window (PCMW)^{60,61} technique to illustrate the dynamic hydration behavior of PVCL, and finally molecular dynamics simulation is also performed to help in our interpretation of the hydrophilic character of the outer surface of PVCL mesoglobules.

2. EXPERIMENTAL SECTION

2.1. Materials. *N*-Vinylcaprolactam (VCL) was purchased from Aladdin Reagent Co. and used as received. Azobis(isobutyronitrile) (AIBN) was also purchased from Aladdin Reagent Co. and recrystallized from ethanol. Methanol was vacuum distilled from calcium hydride before use. PVCL was synthesized by radical polymerization in methanol using AIBN as an initiator. After three freeze–pump–thaw cycles, the polymerization reaction proceeded at $70\text{ }^\circ\text{C}$ for 4 h under nitrogen protection. The synthesized polymer was purified by reprecipitation in hexane twice and further vacuum-dried for 24 h. The number-average molecular weight of PVCL, $M_n = 2.0 \times 10^3$, and polydispersity index $M_w/M_n = 1.35$ were determined by GPC measurements with monodisperse polystyrene as standard and THF as eluent phase at $35\text{ }^\circ\text{C}$. Our synthesized PVCL seems to be an oligomer with a slightly higher LCST than physiological temperature.

D_2O was purchased from Cambridge Isotope Laboratories Inc. (D 99.9%). For Fourier transform infrared (FT-IR) and calorimetric measurements, the concentration of PVCL in water was fixed to 10 wt %. PVCL solution in D_2O was placed at $4\text{ }^\circ\text{C}$ for at least 3 days before FT-IR measurements to ensure complete dissolution.

2.2. Instruments and Measurements. Calorimetric measurements were performed on a Mettler-Toledo differential scanning calorimeter (DSC) thermal analyzer. The sample of PVCL solution for FT-IR measurements was prepared by being sealed between two CaF_2 tablets. All time-resolved FT-IR spectra at different temperatures were recorded on a Nicolet Nexus 470 spectrometer with a resolution of 4 cm^{-1} , and 32 scans were available for an acceptable signal-to-noise ratio. Temperatures were manually controlled with an electronic cell holder at rates of ca. $0.3\text{ }^\circ\text{C}/\text{min}$ with an increment of $0.5\text{ }^\circ\text{C}$. Raw spectra were baseline corrected by the software Omnic, version 6.1a.

2.3. Investigation Methods. **2.3.1. Perturbation Correlation Moving Window.** FT-IR spectra collected with an increment of $0.5\text{ }^\circ\text{C}$ during heating and cooling were used to perform PCMW analysis. Primary data processing was carried out with the method Morita provided, and further correlation calculation was performed using the software 2D Shige, version 1.3 (Shigeaki Morita, Kwansei-Gakuin University, Japan, 2004–2005). The final contour maps were plotted by Origin program, version 8.1, with warm colors (red and yellow) defined as positive intensities and cool colors (blue) defined as negative ones. An appropriate window size ($2m + 1 = 13$) was chosen to generate PCMW spectra with good quality.

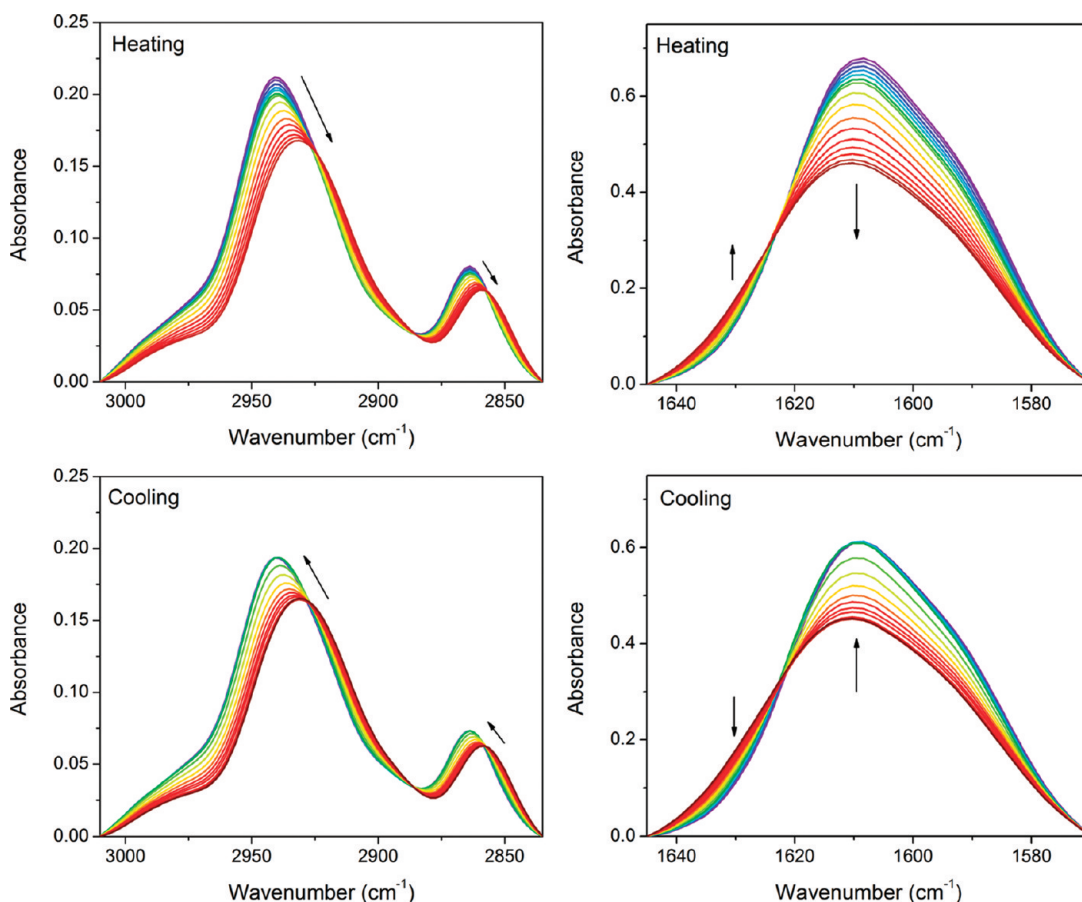


Figure 2. Temperature-dependent FT-IR spectra of PVCL in D_2O (10 wt %) during heating and cooling between 35 and 50 $^{\circ}\text{C}$ in the regions 3010–2835 and 1645–1570 cm^{-1} . For clarity, only a 2 $^{\circ}\text{C}$ interval is shown here.

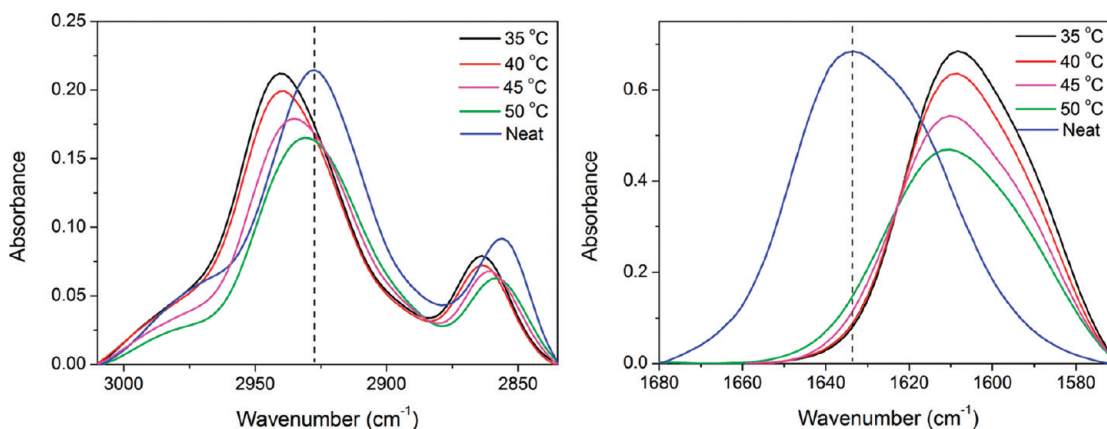


Figure 3. Spectral comparison of PVCL in D_2O (10 wt %) at 35, 40, 45, and 50 $^{\circ}\text{C}$ during heating and neat PVCL sample.

2.3.2. Two-Dimensional Correlation Spectroscopy. FT-IR spectra used for PCMW analysis were also used to perform 2D correlation analysis. Two-dimensional correlation analysis was carried out using the same software 2D Shigeaki Morita, Kwansei-Gakuin University, Japan, 2004–2005), and was further plotted into the contour maps by the Origin program, version 8.1. In the contour maps, warm colors (red and yellow) are defined as positive intensities, while cool colors (blue) are defined as negative ones.

2.3.3. Molecular Dynamics Simulation. All the conformers of model molecules were constructed in the software package Materials

Studio, version 5.0 (Accelrys Inc, San Diego, CA, USA, 2009). The geometry optimization and potential energy calculation were accounted for by the COMPASS force field, which was implemented in the Discover and Forcite modules, respectively.

3. RESULTS AND DISCUSSION

3.1. Calorimetric Measurements. Figure 1 presents the typical DSC curves of PVCL aqueous solution during a heating and cooling cycle. Due to the relatively low molecular weight of

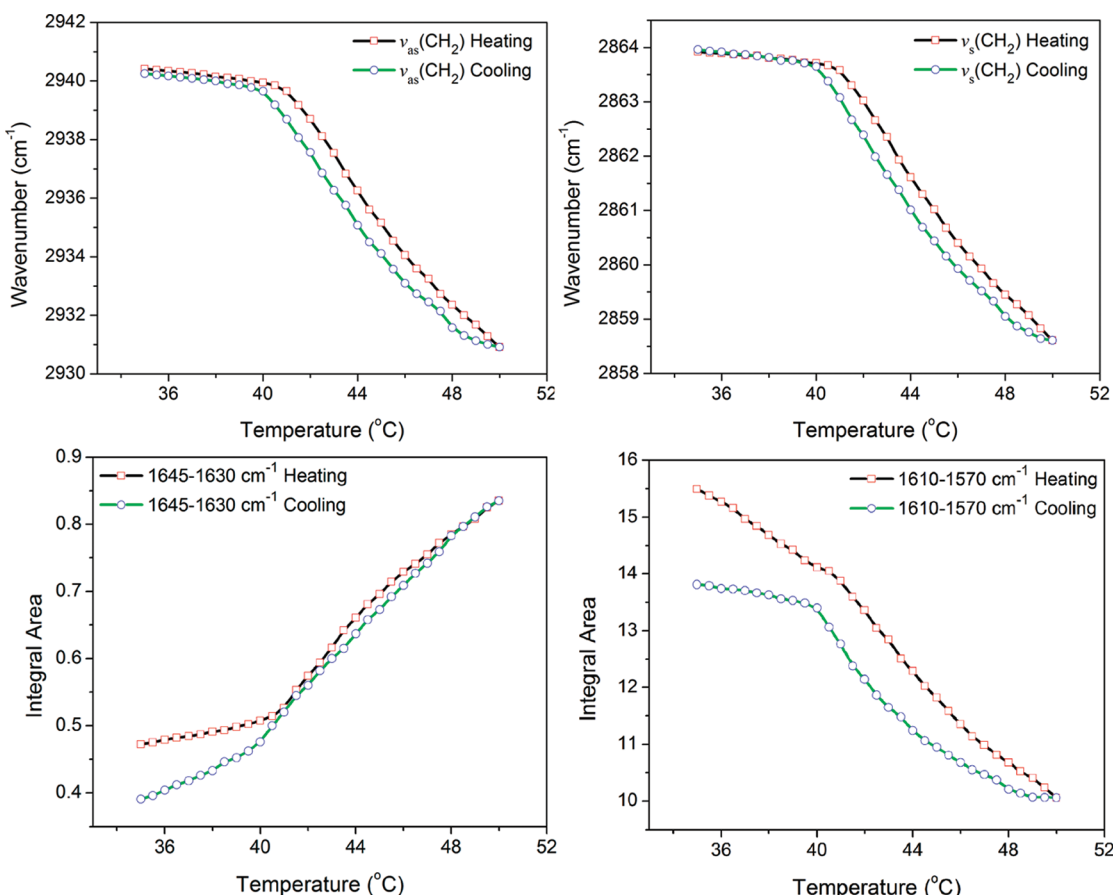


Figure 4. Temperature-dependent frequency shifts of $\nu_{\text{as}}(\text{CH}_2)$ and $\nu_s(\text{CH}_2)$ as well as the integral area in the regions 1645–1630 and 1610–1570 cm^{-1} during heating and cooling, respectively.

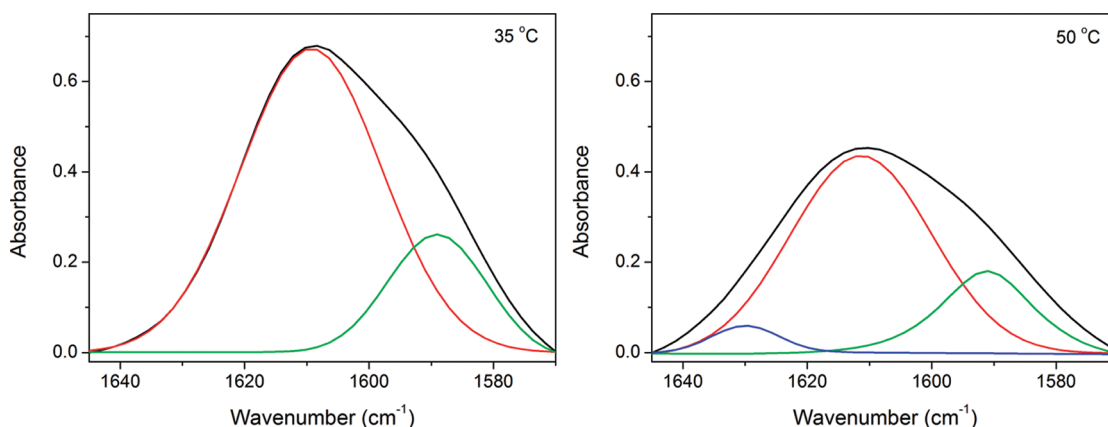


Figure 5. Curve fitted spectra of amide I with different components at 35 °C (1610 and 1592 cm^{-1}) and 50 °C (1633, 1610, and 1592 cm^{-1}), respectively.

the sample we used, the LCST measured by DSC (reflected by the transition temperature at the peak here, 41.1 °C during heating and 37.8 °C during cooling) is a little higher than physiological temperature (~37 °C). From Figure 1 we can find that both heating and cooling DSC curves of PVCL solution are broad (more than 15 °C) and markedly asymmetric with a sharp change below LCST and a gradual change above LCST. As reported, the shape of DSC curves cannot be affected by changing

concentration, molecular weight, and scanning rates, and they can be reproduced during the second and third heating and cooling cycles.⁴⁵ Obviously it cannot be roughly corresponded to the previously reported two successive cooperative transitions (microsegregation and gel volume collapse) in PVCL hydrogels which show a shoulder on the low-temperature side of DSC curves.⁶² It is also considered that a polymer with the demixing temperature strongly dependent on concentration has a broader

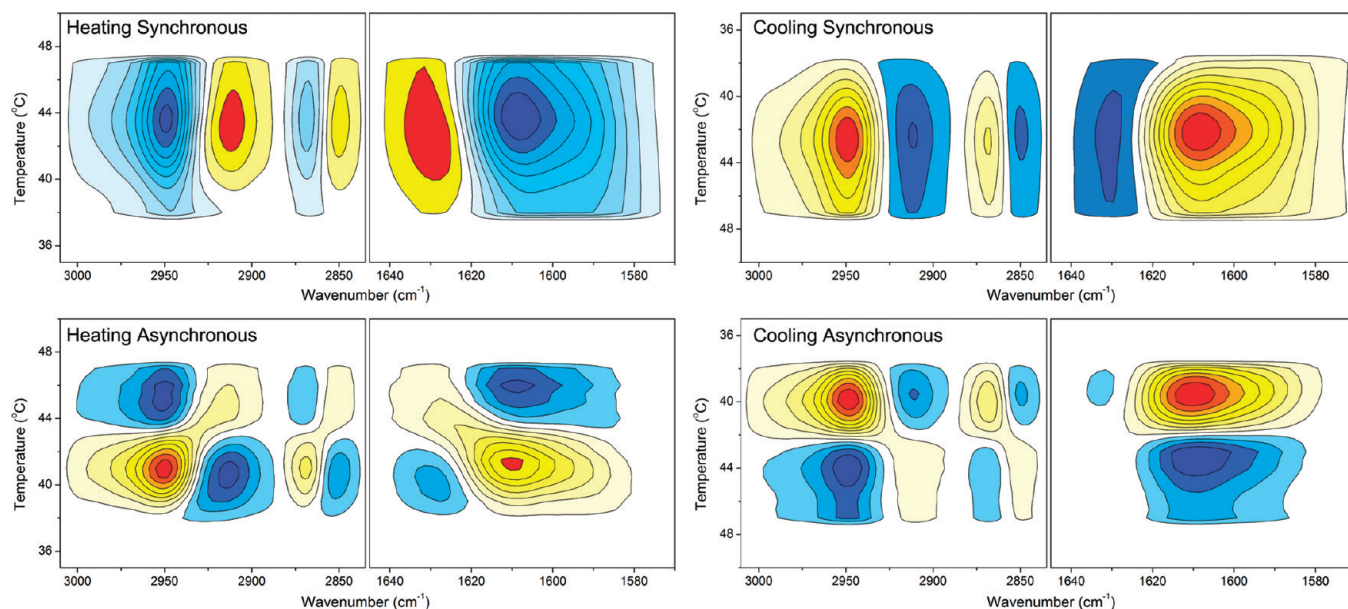


Figure 6. PCMW synchronous and asynchronous spectra of PVCL in D_2O (10 wt %) during heating and cooling between 35 and 50 $^{\circ}\text{C}$, respectively. Herein, warm colors (red and yellow) are defined as positive intensities, while cool colors (blue) are defined as negative ones.

DSC peak.¹⁷ However, none of the previous reports can explain well the two distinct enthalpy changes at the molecular level below and above LCST, which may be the key to understanding the dynamic nature of the continuous phase transition of PVCL in water, since PNIPAM shows a single sharp endotherm peak during heating with a width at half-peak of 2.0 $^{\circ}\text{C}$.⁴⁵

3.2. Conventional IR Analysis. To further understand the asymmetric DSC curves around LCST we observed in calorimetric measurements, temperature-dependent FT-IR spectra of PVCL in D_2O (10 wt %) during one heating and cooling cycle between 35 and 50 $^{\circ}\text{C}$ were measured, as shown in Figure 2. It should be noted that we used D_2O instead of H_2O as the solvent here in order to eliminate the overlap of the $\delta(\text{O}-\text{H})$ band of H_2O around 1640 cm^{-1} with $\nu(\text{C}=\text{O})$ of PVCL as well as the broad $\nu(\text{O}-\text{H})$ band of H_2O around 3300 cm^{-1} with $\nu(\text{C}-\text{H})$ bands of PVCL.¹² As reported, the transition temperature of PVCL in D_2O is only slightly lower than that in H_2O .⁴⁵ Thus, the deuterium isotope effect does not cause obvious changes in the magnitude of hysteresis.

In this paper, two spectral regions are focused on— $\text{C}-\text{H}$ related stretching vibrations (3010–2835 cm^{-1}) and $\text{C}=\text{O}$ related stretching vibrations (amide I, 1645–1570 cm^{-1})—which can be used to trace nearly all group motions of PVCL. Examining carefully the spectral variations in Figure 2, we can find that during heating all the $\text{C}-\text{H}$ stretching bands shift to lower frequency, while $\text{C}=\text{O}$ exhibits a binary spectral intensity change. During cooling the case is just opposite that in the heating process.

To discern the effect of hydration on the frequency of $\text{C}-\text{H}$ and $\text{C}=\text{O}$ stretching bands, spectral comparison of PVCL in D_2O at four different temperatures and neat PVCL has been presented in Figure 3. Since neat PVCL cannot form hydrophobic hydration and hydrogen bonding due to the absence of proton in amide groups, we can ascribe the $\text{C}-\text{H}$ groups and amide groups to be free of water and hydrogen bonds, respectively. Thus, the changes of $\nu(\text{C}-\text{H})$ bands during heating can be explained by a gradual hydrophobic hydration of PVCL with

neighboring water molecules. The higher the number of water molecules surrounding $\text{C}-\text{H}$ groups is, the higher the vibrational frequency is.⁶³ However, we can find that, after the phase transition (>45 $^{\circ}\text{C}$), $\text{C}-\text{H}$ groups still exhibit dehydration and cannot be completely free of water even long after the phase transition (50 $^{\circ}\text{C}$). This tendency can be easily observed in temperature-dependent frequency shifts of $\nu_{\text{as}}(\text{CH}_2)$ and $\nu_{\text{s}}(\text{CH}_2)$ in Figure 4. The frequency of the $\text{C}-\text{H}$ stretching bands shows a sharp shift below LCST and a gradual shift above LCST, which exhibits a typical asymmetric sigmoid curve, also in good conformity with above DSC observations. Note that PNIPAM has the frequency nearly unchanged both before and after phase transition (typical symmetric sigmoid curve); this proves that PVCL has a reduced magnitude of conformation changes due to topological constraints of caprolactam rings compared to PNIPAM,¹² which has also been observed by fluorescence investigations.⁴⁸

The changes of amide I during heating can be explained by the transformation of hydrogen bonded $\text{C}=\text{O}$ with water to free ones, determined from the presence of characterized vibrations of free $\text{C}=\text{O}$ (around 1634 cm^{-1}) in both neat PVCL and PVCL solution after phase transition (>45 $^{\circ}\text{C}$). Similarly, the number of free and hydrogen bonded carbonyls also shows a sharp change below LCST and a gradual change above LCST, reflected by the integral area in the regions 1645–1630 and 1610–1570 cm^{-1} , respectively. The gradual changes of $\text{C}-\text{H}$ and $\text{C}=\text{O}$ related bands strongly prompt us to believe that there may exist a distribution gradient of water molecules in PVCL mesoglobules. With further increase of the temperature, more water molecules are expelled outside resulting in more collapsed chains.

It is also notable that amide I consists of more than one type of hydrogen bonded carbonyls, as shown in Figure 5. After phase transition, a new band around 1633 cm^{-1} corresponding to free carbonyls appeared. According to Maeda et al., the existence of a larger number of components of carbonyls in PVCL than in PNIPAM can be attributed to the less localized *cis*-amide group in a cyclic caprolactam ring, which would be easily affected by the

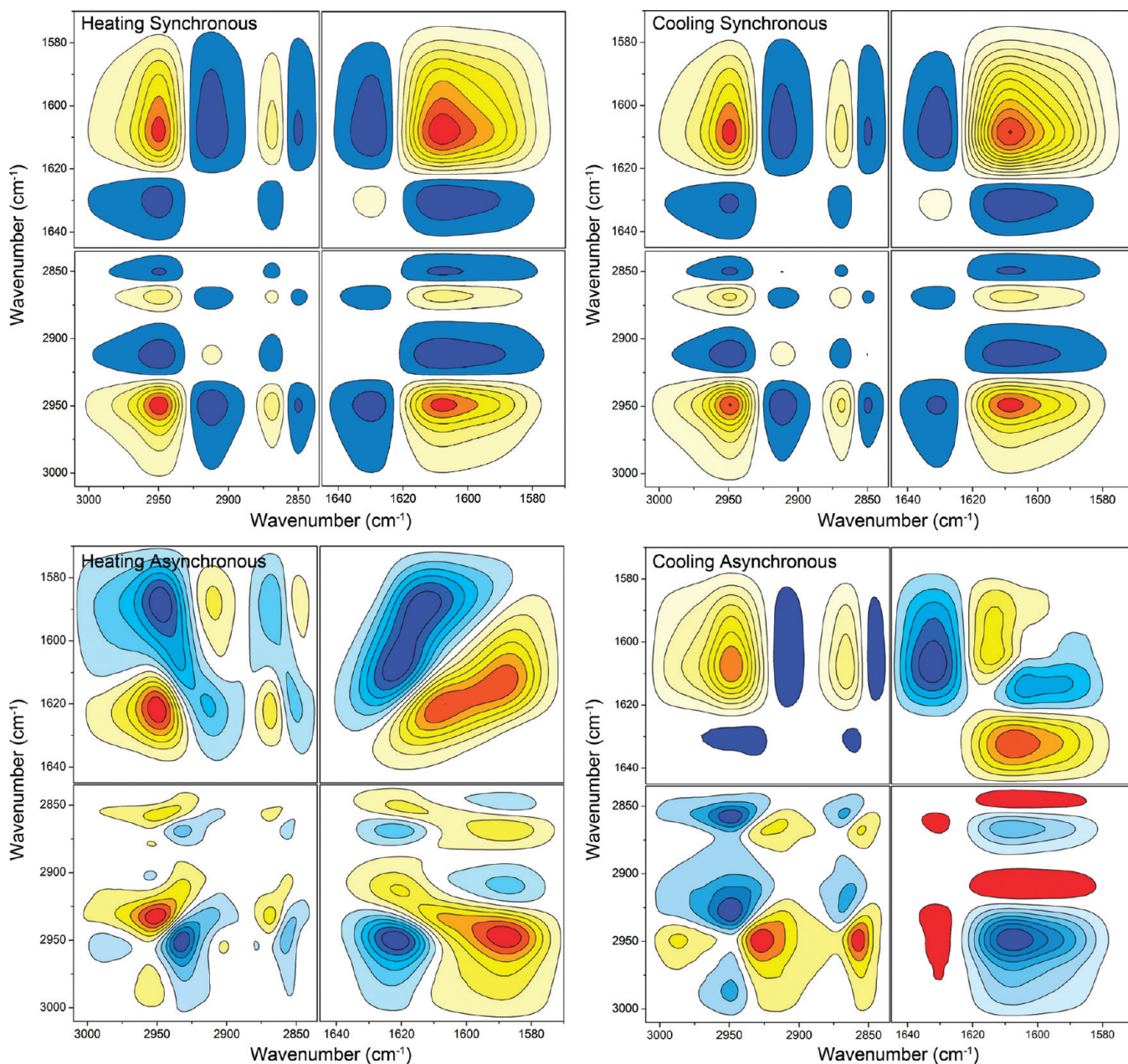


Figure 7. 2DCOS synchronous and asynchronous spectra of PVCL in D₂O (10 wt %) during heating and cooling between 39.5 and 45 °C, respectively. Herein, warm colors (red and yellow) are defined as positive intensities, while cool colors (blue) are defined as negative ones.

hydrogen bonding state while a *trans*-amide group in PNIPAM is more localized.¹⁷

As for the asymmetric sigmoid curves in Figure 4, it is hard to accurately determine the transition temperatures during heating and cooling, even for our often-used Boltzmann fitting method.¹¹ Thus a PCMW method was employed to help in the determination of transition temperatures and ranges.

3.3. Perturbation Correlation Moving Window. PCMW is a newly developed technique, whose basic principles can date back to the conventional moving window proposed by Thomas,⁶⁰ and later in 2006 Morita⁶¹ improved this technique to much wider applicability through introducing a perturbation variable into the correlation equation. Together with its original ability in determining transition points as the

conventional moving window did, PCMW can additionally monitor complicated spectral variations along the perturbation direction.

Figure 6 presents PCMW synchronous and asynchronous spectra of PVCL in D₂O during heating and cooling between 35 and 50 °C, respectively. PCMW synchronous spectra are very helpful to find transition points. Thus for all C–H and C=O related bands, LCST is ca. 43.5 °C during heating and ca. 42.5 °C during cooling, suggesting an apparent hysteresis phenomenon. All the groups (mainly side groups detected by PCMW) do not exhibit obvious differences in responding temperatures during both heating and cooling, indicating that the side groups of PVCL have good coordination of group motions due to strong covalent binding in the caprolactam ring.

Table 1. Tentative Band Assignments of PVCL in D₂O According to 2DCOS Results^{10,11,17}

wavenumber/cm ⁻¹	assignment	wavenumber/cm ⁻¹	assignment
2987	ν_{as} (CH ₂ , linking to C=O)	1632	ν (free C=O)
2952	ν_{as} (hydrated CH ₂ , away from C=O)	1620	ν (hydrogen bonded C=O)
2930	ν_{as} (dehydrated CH ₂ , away from C=O)	1614	
2898	ν (CH, backbone)	1608	
2879	ν_s (CH ₂ , linking to C=O)	1600	
2870	ν_s (hydrated CH ₂ , away from C=O)	1589	
2856	ν_s (dehydrated CH ₂ , away from C=O)		

In addition to determining transition points, PCMW can also monitor the spectral variations along temperature perturbation, combining the signs of synchronous and asynchronous spectra by the following rules: a positive synchronous correlation represents spectral intensity increasing, while a negative one represents spectral intensity decreasing; a positive asynchronous correlation can be observed for a convex spectral intensity variation while a negative one can be observed for a concave variation.⁶¹ On the basis of this point, we can ascertain that both C—H and C=O related vibrations of PVCL show S-shaped or anti-S-shaped spectral changes, consistent with the above conventional IR analysis. The transition temperature region can also be determined by the peaks in asynchronous spectra, which are all turning points of the sigmoid curves. Then we can conclude that PVCL experiences phase transition in D₂O mainly between 40.5 and 45 °C during heating and between 39.5 and 44 °C during cooling. This served as an important basis for the segmental mode of the following 2DCOS analysis.

3.4. Two-Dimensional Correlation Analysis. 2DCOS is a mathematical method whose basic principles were first proposed by Noda in 1986.⁵⁸ Up to the present time, 2DCOS has been widely used to study spectral variations of different chemical species under various external perturbations (temperature, pressure, concentration, time, electromagnetic, etc).⁵⁹ Due to the different response of different species to external variables, additional useful information about molecular motions or conformational changes can be extracted which cannot be obtained straight from conventional one-dimensional spectra.

On the basis of the phase transition evolving regions obtained from PCMW, we chose all the spectra between 39.5 and 45 °C to perform 2DCOS analysis, as shown in Figure 7. Two-dimensional synchronous spectra reflect simultaneous changes between two given wavenumbers. The bands at 2952, 2870, and 1608 cm⁻¹ all have positive cross-peaks, indicating that they had similar responses of spectral intensities to temperature perturbation: that is, all decrease during heating and all increase during cooling determined from raw spectra. On the other hand, the bands at 2987, 2856, and 1633 cm⁻¹ have spectral intensities both increasing during heating and decreasing during cooling.

Two-dimensional asynchronous spectra can significantly enhance the spectral resolution. In Figure 7, many subtle bands during heating such as the bands at 2987, 2930, and 2898 cm⁻¹ attributed to ν_{as} (dehydrated CH₂) and ν (CH) as well as six C=O splitting bands at 1633, 1620, 1614, 1608, 1600, and 1589 cm⁻¹ have been identified. For the convenience of discussion, all the bands found in asynchronous spectra and their corresponding assignments have been presented in Table 1.

Table 2. Final Results of Multiplication on the Signs of Each Cross-Peak in Synchronous and Asynchronous Spectra during Heating and Cooling, Respectively

Heating												
	2987	2952	2930	2898	2879	2870	2856	1620	1614	1608	1589	
1589	—	—	—	—	—	—	—	—	—	—	—	—
1608	—	—	—	—	—	—	—	+	—	—	—	—
1614	+	+	—	+	+	+	+	+	—	—	—	—
1620	+	+	+	+	+	+	+	+	+	—	—	—
2856	—	—	—	—	—	—	—	—	—	—	—	—
2870	—	+	—	—	—	—	—	—	—	—	—	—
2879	+	—	—	+	—	—	—	—	—	—	—	—
2898	—	+	—	—	—	—	—	—	—	—	—	—
2930	+	+	—	—	—	—	—	—	—	—	—	—
2952	—	—	—	—	—	—	—	—	—	—	—	—
2987	—	—	—	—	—	—	—	—	—	—	—	—

Cooling												
	2987	2952	2930	2898	2870	2856	1632	1614	1608	1600		
1600	+	+	+	+	+	+	—	+	+	+	+	—
1606	+	+	+	—	+	—	—	+	+	+	+	—
1614	+	+	+	—	+	—	—	—	+	—	—	—
1632	+	+	+	—	+	—	—	—	—	—	—	—
2856	+	+	+	+	+	+	—	—	—	—	—	—
2870	+	—	+	—	—	—	—	—	—	—	—	—
2898	+	+	+	—	—	—	—	—	—	—	—	—
2930	—	—	—	—	—	—	—	—	—	—	—	—
2952	+	—	—	—	—	—	—	—	—	—	—	—
2987	—	—	—	—	—	—	—	—	—	—	—	—

Except for enhancing spectral resolution, 2DCOS can also discern the specific order taking place under external perturbation. The judging rule can be summarized as Noda's rule: that is, if the cross-peaks (ν_1 , ν_2 , and assume $\nu_1 > \nu_2$) in synchronous and asynchronous spectra have the same sign, the change at ν_1 may occur prior to that of ν_2 , and vice versa. A simplified method for the determination of sequence order has been described before.⁶⁴ In short, multiplication was performed on the two signs of each cross-peak in synchronous and asynchronous spectra, the final results of which have been presented in Table 2. For each sign of the cross-peaks in Table 2, according to Noda's rule, if the sign is positive (+), the larger wavenumber or the bottom wavenumber will respond to external perturbation earlier than the smaller wavenumber or the left wavenumber. Similarly, if the sign is negative (-), the left wavenumber will respond earlier than the bottom one. If the sign is zero (or blank), we cannot make an

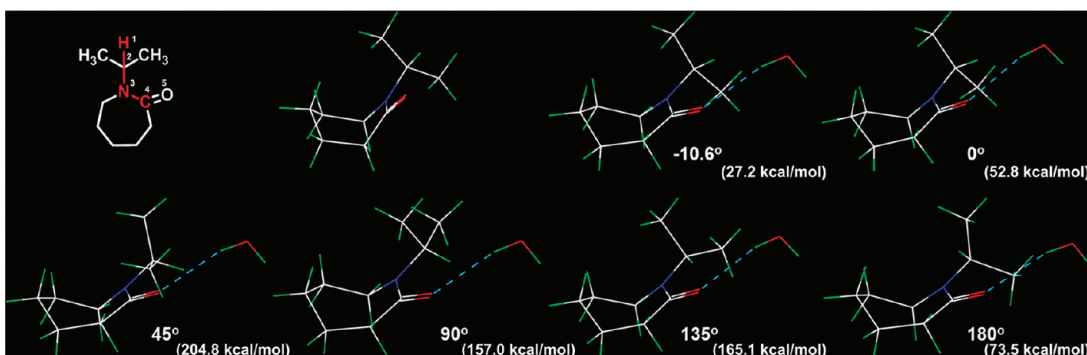


Figure 8. Chemical structure of *N*-isopropylcaprolactam and its six conformers associated with one water molecule by varying the dihedral angle ($\text{H}1-\text{C}2-\text{N}3-\text{C}4$) to be -10.6° , 0° , 45° , 90° , 135° , and 180° . The conformer with the dihedral angle of -10.6° is the optimized one. The values in parentheses are the calculated potential energies of corresponding conformers. Red represents O atoms while green represents H atoms and gray white represents C atoms.

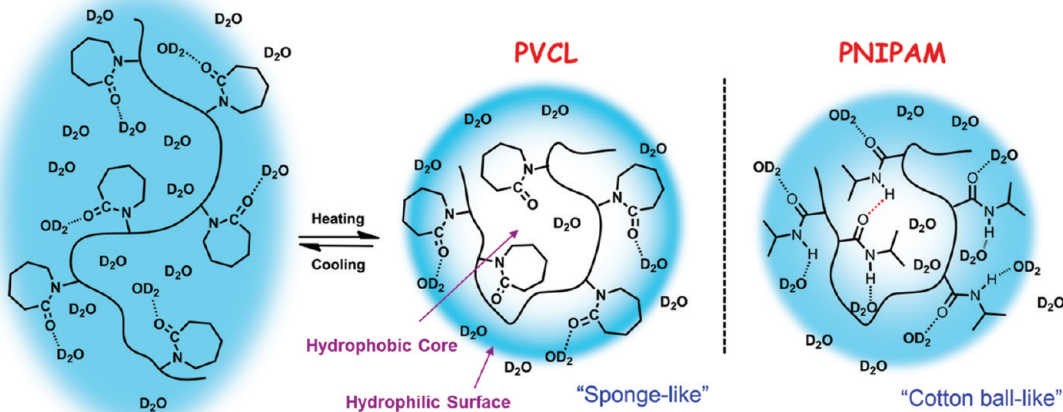


Figure 9. Schematic illustration of the dynamic hydration behavior of PVCL and the structural comparison between “sponge-like” PVCL mesoglobules and “cotton-ball-like” PNIPAM mesoglobules. The light blue color represents the distribution density of water molecules.

exact judgment. Thus we can easily deduce the final specific order for the heating process of PVCL in D₂O (“→” means prior to or earlier than): $1589\text{ cm}^{-1} \rightarrow 2856\text{ cm}^{-1} \rightarrow 1608\text{ cm}^{-1} \rightarrow 2952\text{ cm}^{-1} \rightarrow 2870\text{ cm}^{-1} \rightarrow 2898\text{ cm}^{-1} \rightarrow 2879, 2987\text{ cm}^{-1} \rightarrow 1614\text{ cm}^{-1} \rightarrow 2930\text{ cm}^{-1} \rightarrow 1620\text{ cm}^{-1}$.

Considering separately C=O related vibrations, the sequence can be extracted as follows: $1589\text{ cm}^{-1} \rightarrow 1608\text{ cm}^{-1} \rightarrow 1614\text{ cm}^{-1} \rightarrow 1620\text{ cm}^{-1}$. Interestingly, the frequency of C=O related vibrations exhibits a gradual increase, indicating the gradual weakening of hydrogen bonds during heating, which may further confirm our previous deduction about the existence of a distribution gradient of water molecules in PVCL mesoglobules.

Not considering the differences of vibration modes of C-H and C=O groups, we have C=O → C-H. This reveals that the phase transition of PVCL during heating is driven by hydrogen bonding transformation of amide groups, followed by the hydrophobic dehydration of C-H groups. Thus it is reasonable that hydrophobic interaction predominates at the second stage of phase transition above LCST, which shows gradual changes upon further increase of the temperature, while hydrogen bonding transformation predominates at the first stage below LCST with sharp changes.

Similarly, the sequence order for the cooling process of PVCL in D₂O can be deduced: $2930\text{ cm}^{-1} \rightarrow 2987\text{ cm}^{-1} \rightarrow 2870\text{ cm}^{-1} \rightarrow 2952\text{ cm}^{-1} \rightarrow 1632\text{ cm}^{-1} \rightarrow 1614\text{ cm}^{-1} \rightarrow 1608\text{ cm}^{-1} \rightarrow 2898\text{ cm}^{-1} \rightarrow 1600\text{ cm}^{-1} \rightarrow 2856\text{ cm}^{-1}$. Considering separately C=O related vibrations, we have $1632\text{ cm}^{-1} \rightarrow 1614\text{ cm}^{-1} \rightarrow 1608\text{ cm}^{-1} \rightarrow 1600\text{ cm}^{-1}$. It is notable that the frequency of C=O related vibrations exhibits a gradual decrease, indicating the gradual formation of hydrogen bonds during cooling, which is also evident for the existence of a distribution gradient of water molecules in PVCL mesoglobules. Not considering the differences of vibration modes of C-H and C=O groups, we just have the opposite order during cooling: C-H → C=O. Thus the phase transition during cooling can be seen as the inverse process during heating, driven by the hydrophobic hydration of C-H groups, followed by hydrogen bonding transformation of amide groups.

Note that the overall frequencies of amide I according to 2DCOS during cooling are higher than those during heating. This reveals that more disordered water associates are formed during cooling than in the original state during heating, which is also consistent with a previous report that PVCL is a rather poorer structure maker than PNIPAM.⁴⁵ In addition, the side

groups of PVCL always have an earlier response than backbones during both heating and cooling, which can be attributed to their relatively larger degree of freedom.

3.5. Molecular Dynamics Simulation. To further interpret the structure of PVCL mesoglobules, we performed molecular dynamics simulation. *N*-Isopropylcaprolactam was chosen to be the model molecule of PVCL repeat units, in which the isopropyl group can represent the backbone of PVCL. The optimized structure of *N*-isopropylcaprolactam with a dihedral angle ($C_2-N_3-C_4-O_5$) of 2.9° is shown in Figure 8. The addition of one water molecule changed this dihedral angle to 6.1° , which may account for the easily affected less localized *cis*-amide groups of PVCL by the hydrogen bonding state resulting in large numbers of components observed by IR spectroscopy. The conformer with the dihedral angle ($H_1-C_2-N_3-C_4$) of -10.6° is the optimized one with the lowest potential energy, in which the water molecule is nearly perpendicular to the isopropyl group. As this dihedral angle varies from 0° to 180° , the conformer becomes unstable always when the water molecule is more or less parallel to the isopropyl group. This reveals that the "chair" caprolactam ring of PVCL should have amide groups outside when the backbones collapse to form mesoglobules, which also support the hydrophilic character of the outer surface of PVCL.

In combination with our above IR analysis, we can conclude that there exists a distribution gradient of water molecules in PVCL mesoglobules ranging from a hydrophobic core to a hydrophilic surface. Therefore we draw the schematic dynamic hydration behavior of PVCL in D_2O during heating and cooling, as shown in Figure 9. Herein, due to the absence of self-associated hydrogen bonds and topological constraints, PVCL mesoglobules would form a "sponge-like" structure which can further continuously expel water molecules upon increasing temperature. PNIPAM with self-associated hydrogen bonds forms mesoglobules exhibiting a "cotton-ball-like" structure without an apparent distribution gradient of water molecules and does not change much upon increasing temperature. The "sponge-like" structure of PVCL has also been reported by a high-resolution SANS investigation.⁴⁷ In addition, the distribution gradient of water molecules in PVCL mesoglobules may be closely related to the different diffusion coefficients of polymer chains between the core and the surface,⁶⁵ which may need to be further discussed.

4. CONCLUSION

In this paper, FT-IR spectroscopy, calorimetric measurements, and molecular dynamics simulation were employed to elucidate the dynamic hydration behavior of PVCL in D_2O (10 wt %). DSC curves of PVCL aqueous solution are broad and markedly asymmetric during both heating and cooling with a sharp change below LCST and a gradual change above LCST. This phenomenon can also be observed by the temperature-dependent frequency shifts of C–H groups and the integral area of amide groups in conventional IR analysis, indicating that PVCL has a reduced magnitude of conformation changes due to topological constraints of caprolactam rings compared to PNIPAM. Moreover, PCMW easily determined the transition temperature to be $43.5\text{ }^\circ\text{C}$ during heating and $42.5\text{ }^\circ\text{C}$ during cooling as well as the transition temperature range between 39.5 and $45\text{ }^\circ\text{C}$. 2DCOS was used to discern the sequence order of different species in PVCL and attributed the hydrogen bonding transformation as predominant at the first transition stage below LCST and hydrophobic interaction to be predominant at the second transition stage above LCST. Finally, in combination with

molecular dynamics simulation of a model molecule of PVCL repeat units, we concluded that there exists a distribution gradient of water molecules in PVCL mesoglobules ranging from a hydrophobic core to a hydrophilic surface. Additionally, due to the absence of self-associated hydrogen bonds and topological constraints, PVCL mesoglobules would form a "sponge-like" structure which can further continuously expel water molecules upon increasing temperature. PNIPAM with self-associated hydrogen bonds forms mesoglobules exhibiting a "cotton-ball-like" structure without an apparent distribution gradient of water molecules and does not change much with increasing temperature.

■ AUTHOR INFORMATION

Corresponding Author

*E-mail: peiyiwu@fudan.edu.cn.

■ ACKNOWLEDGMENT

We gratefully acknowledge financial support from the National Science Foundation of China (NSFC) (Nos. 20934002, 51073043) and the National Basic Research Program of China (No. 2009CB930000).

■ REFERENCES

- (1) Liu, F.; Urban, M. W. *Prog. Polym. Sci.* **2010**, *35*, 3.
- (2) Qiu, Y.; Park, K. *Adv. Drug Delivery Rev.* **2001**, *53*, 321.
- (3) Yu, L.; Ding, J. *Chem. Soc. Rev.* **2008**, *37*, 1473.
- (4) Kim, J.; Park, K. *Bioseparation* **1998**, *7*, 177.
- (5) Schäfer-Soenen, H.; Moerkerke, R.; Berghmans, H.; Koningsveld, R.; Dušek, K.; Šolc, K. *Macromolecules* **1997**, *30*, 410.
- (6) Moerkerke, R.; Meeussen, F.; Koningsveld, R.; Berghmans, H.; Mondelaers, W.; Schacht, E.; Dušek, K.; Šolc, K. *Macromolecules* **1998**, *31*, 2223.
- (7) Meeussen, F.; Nies, E.; Berghmans, H.; Verbrugghe, S.; Goethals, E.; Du Prez, F. *Polymer* **2000**, *41*, 8597.
- (8) Ono, Y.; Shikata, T. *J. Am. Chem. Soc.* **2006**, *128*, 10030.
- (9) Zhou, K.; Lu, Y.; Li, J.; Shen, L.; Zhang, G.; Xie, Z.; Wu, C. *Macromolecules* **2008**, *41*, 8927.
- (10) Sun, B.; Lin, Y.; Wu, P.; Siesler, H. W. *Macromolecules* **2008**, *41*, 1512.
- (11) Sun, S.; Hu, J.; Tang, H.; Wu, P. *J. Phys. Chem. B* **2010**, *114*, 9761.
- (12) Sun, S.; Wu, P. *Macromolecules* **2010**, *43*, 9501.
- (13) Du, H.; Wickramasinghe, R.; Qian, X. *J. Phys. Chem. B* **2010**, *114*, 16594.
- (14) Guo, Y.; Sun, B.; Wu, P. *Langmuir* **2008**, *24*, 5521.
- (15) Sun, B.; Lai, H.; Wu, P. *J. Phys. Chem. B* **2011**, *115*, 1335.
- (16) Spěváček, J. i.; Hanyková, L.; Labuta, J. *Macromolecules* **2011**, *44*, 2149.
- (17) Maeda, Y.; Nakamura, T.; Ikeda, I. *Macromolecules* **2002**, *35*, 217.
- (18) Wei, H.; Cheng, S. X.; Zhang, X. Z.; Zhuo, R. X. *Prog. Polym. Sci.* **2009**, *34*, 893.
- (19) Karg, M.; Hellweg, T. *Curr. Opin. Colloid Interface Sci.* **2009**, *14*, 438.
- (20) Álvarez-Puebla, R. A.; Contreras-Cáceres, R.; Pastoriza-Santos, I.; Pérez-Juste, J.; Liz-Marzáñ, L. M. *Angew. Chem., Int. Ed.* **2009**, *48*, 138.
- (21) Kostanski, L. K.; Huang, R. X.; Ghosh, R.; Filipe, C. D. M. *J. Biomater. Sci. Polym. Ed.* **2008**, *19*, 275.
- (22) Vihola, H.; Laukkonen, A.; Valtola, L.; Tenhu, H.; Hirvonen, J. *Biomaterials* **2005**, *26*, 3055.
- (23) Okhapkin, I. M.; Nasimova, I. R.; Makhaeva, E. E.; Khokhlov, A. R. *Macromolecules* **2003**, *36*, 8130.
- (24) Prabaharan, M.; Grailer, J. J.; Steeber, D. A.; Gong, S. Q. *Macromol. Biosci.* **2009**, *9*, 744.

- (25) Galant, C.; Kjoniksen, A. L.; Knudsen, K. D.; Helgesen, G.; Lund, R.; Laukkonen, A.; Tenhu, H.; Nystrom, B. *Langmuir* **2005**, *21*, 8010.
- (26) Kozlovskaya, V.; Shamaev, A.; Sukhishvili, S. A. *Soft Matter* **2008**, *4*, 1499.
- (27) Alzari, V.; Monticelli, O.; Nuvoli, D.; Kenny, J. M.; Marian, A. *Biomacromolecules* **2009**, *10*, 2672.
- (28) Pich, A.; Tessier, A.; Boyko, V.; Lu, Y.; Adler, H. J. P. *Macromolecules* **2006**, *39*, 7701.
- (29) Schachschal, S.; Balaceanu, A.; Melian, C.; Demco, D. E.; Eckert, T.; Richtering, W.; Pich, A. *Macromolecules* **2010**, *43*, 4331.
- (30) Balaceanu, A.; Demco, D. E.; Moller, M.; Pich, A. *Macromolecules* **2011**, *44*, 2161.
- (31) Erel-Unal, I.; Sukhishvili, S. A. *Macromolecules* **2008**, *41*, 8737.
- (32) Zhuk, A.; Pavlukhina, S.; Sukhishvili, S. A. *Langmuir* **2009**, *25*, 14025.
- (33) Pich, A.; Hain, J.; Lu, Y.; Boyko, V.; Prots, Y.; Adler, H. J. *Macromolecules* **2005**, *38*, 6610.
- (34) Agrawal, M.; Pich, A.; Gupta, S.; Zafeiropoulos, N. E.; Rubio-Retama, J.; Simon, F.; Stamm, M. *J. Mater. Chem.* **2008**, *18*, 2581.
- (35) Karg, M.; Hellweg, T. *J. Mater. Chem.* **2009**, *19*, 8714.
- (36) Imaz, A.; Forcada, J. *J. Polym. Sci., Part A: Polym. Chem.* **2010**, *48*, 1173.
- (37) Markovicheva, E. A.; Kuptsova, S. V.; Mareeva, T. Y.; Vikhrov, A. A.; Dugina, T. N.; Strukova, S. M.; Belokon, Y. N.; Kochetkov, K. A.; Baranova, E. N.; Zubov, V. P.; Poncelet, D.; Parmar, V. S.; Kumar, R.; Rumsh, L. D. *Appl. Biochem. Biotechnol.* **2000**, *88*, 145.
- (38) Lee, E. M.; Gwon, S. Y.; Ji, B. C.; Bae, J. S.; Kim, S. H. *Fiber Polym.* **2011**, *12*, 288.
- (39) Miserez, B.; Lynen, F.; Wright, A.; Euerby, M.; Sandra, P. *Chromatographia* **2010**, *71*, 1.
- (40) Wahlund, P. O.; Galaev, I. Y.; Kazakov, S. A.; Lozinsky, V. I.; Mattiasson, B. *Macromol. Biosci.* **2002**, *2*, 33.
- (41) Lozinsky, V. I.; Simenel, I. A.; Kulakova, V. K.; Kurskaya, E. A.; Babushkina, T. A.; Klimova, T. P.; Burova, T. V.; Dubovik, A. S.; Grinberg, V. Y.; Galaev, I. Y. *Macromolecules* **2003**, *36*, 7308.
- (42) Lau, A.; Wu, C. *Macromolecules* **1999**, *32*, 581.
- (43) Kirsh, Y. E.; Yanul, N. A.; Kalnins, K. K.; Maslov, V. G. *J. Mol. Liq.* **1999**, *82*, 117.
- (44) Kirsh, Y. E.; Yanul, N. A.; Kalnins, K. K. *Eur. Polym. J.* **1999**, *35*, 305.
- (45) Laukkonen, A.; Valtola, L.; Winnik, F. M.; Tenhu, H. *Macromolecules* **2004**, *37*, 2268.
- (46) Aseyev, V.; Hietala, S.; Laukkonen, A.; Nuopponen, M.; Confortini, O.; Du Prez, F. E.; Tenhu, H. *Polymer* **2005**, *46*, 7118.
- (47) Lebedev, V.; Torok, G.; Cser, L.; Treimer, W.; Orlova, D.; Sibilev, A. *J. Appl. Crystallogr.* **2003**, *36*, 967.
- (48) Chee, C. K.; Rimmer, S.; Soutar, I.; Swanson, L. *React. Funct. Polym.* **2006**, *66*, 1.
- (49) Vorob'ev, M. M.; Burova, T. V.; Grinberg, N. V.; Dubovik, A. S.; Faleev, N. G.; Lozinsky, V. I. *Colloid Polym. Sci.* **2010**, *288*, 1457.
- (50) Vasilevskaya, V. V.; Khalatur, P. G.; Khokhlov, A. R. *Macromolecules* **2003**, *36*, 10103.
- (51) Foroustan, M.; Khoei, S.; Zarrabi, M. *J. Appl. Polym. Sci.* **2008**, *109*, 597.
- (52) Foroustan, M.; Zarrabi, M. *J. Chem. Thermodyn.* **2009**, *41*, 448.
- (53) Tager, A. A.; Safronov, A. P.; Sharina, S. V.; Galaev, I. Y. *Colloid Polym. Sci.* **1993**, *271*, 868.
- (54) Tager, A. A.; Safronov, A. P.; Berezyuk, E. A.; Galaev, I. Y. *Colloid Polym. Sci.* **1994**, *272*, 1234.
- (55) Higuchi, T.; Ikeda, I. *Langmuir* **2000**, *16*, 7503.
- (56) Maeda, Y.; Nakamura, T.; Ikeda, I. *Macromolecules* **2001**, *34*, 8246.
- (57) Cheng, H.; Shen, L.; Wu, C. *Macromolecules* **2006**, *39*, 2325.
- (58) Noda, I. *Bull. Am. Phys. Soc.* **1986**, *31*, 520.
- (59) Noda, I.; Ozaki, Y. *Two-Dimensional Correlation Spectroscopy: Applications in Vibrational and Optical Spectroscopy*; Wiley: New York, 2004.
- (60) Thomas, M.; Richardson, H. H. *Vib. Spectrosc.* **2000**, *24*, 137.
- (61) Morita, S.; Shinzawa, H.; Noda, I.; Ozaki, Y. *Appl. Spectrosc.* **2006**, *60*, 398.
- (62) Mikheeva, L. M.; Grinberg, N. V.; Mashkevich, A. Y.; Grinberg, V. Y.; Thanh, L. T. M.; Makhaeva, E. E.; Khokhlov, A. R. *Macromolecules* **1997**, *30*, 2693.
- (63) Schmidt, P.; Dybal, J.; Trchová, M. *Vib. Spectrosc.* **2006**, *42*, 278.
- (64) Sun, S.; Tang, H.; Wu, P.; Wan, X. *Phys. Chem. Chem. Phys.* **2009**, *11*, 9861.
- (65) Rubio Retama, J.; Frick, B.; Seydel, T.; Stamm, M.; Fernandez Barbero, A.; López Cabarcos, E. *Macromolecules* **2008**, *41*, 4739.